

VARIATION OF BOOSTER TUNES WITH MOMENTUM

S. C. Snowdon

10/29/69

A. PURPOSE

The booster magnet sextupole components were selected to remove the momentum variation of betatron frequencies for small amplitudes and momentum excursion. This note indicates the extent to which this condition is fulfilled using the measured gradients and a momentum range that spans the available aperture.

B. RADIAL MOTION

On the median plane the radial motion is expressed adequately by

$$\frac{d^2x}{ds^2} = \frac{1}{\rho} \left(1 + \frac{x}{\rho}\right) + \frac{e}{p} \left(1 + \frac{x}{\rho}\right)^2 B_Y. \quad (1)$$

Let x be a periodic solution of Eq. (1) and expand radial motion around this solution,

$$x = X + u, \quad (2)$$

retaining only terms linear in the betatron amplitude u .

$$B_Y(x) \equiv B_Y(X) + u B_Y'(X) + \dots \quad (3)$$

$$\frac{1}{\rho} + \frac{e}{p_0} B_Y(0) \equiv 0 \quad (4)$$

$$\frac{p_0}{p} = \frac{p - \Delta p}{p} = 1 - \frac{\Delta p}{p} \quad (5)$$

Then

$$\frac{d^2X}{ds^2} + \frac{d^2u}{ds^2} = \frac{1}{\rho} + \frac{X}{\rho^2} + \frac{u}{\rho^2} - \frac{1}{\rho} \left(1 - \frac{\Delta p}{p}\right) \left(1 + \frac{X}{\rho} + \frac{u}{\rho}\right)^2 \cdot \left(\frac{B_Y(X)}{B_Y(0)} + u \frac{B_Y'(X)}{B_Y(0)} \right). \quad (6)$$

But

$$\frac{d^2X}{ds^2} = \frac{1}{\rho} + \frac{X}{\rho^2} - \frac{1}{\rho} \left(1 - \frac{\Delta p}{p}\right) \left(1 + \frac{X}{\rho}\right)^2 \cdot \frac{B_Y(X)}{B_Y(0)}. \quad (7)$$

Let

$$k_1 = \frac{B_Y'(0)}{B_Y(0)} \quad (8)$$

$$g(X) = \frac{B_Y'(X)}{B_Y'(0)} \quad (9)$$

$$b(X) = \frac{B_Y(X)}{B_Y(0)}. \quad (10)$$

Then, after subtracting Eq. (7) from Eq. (6) and retaining only terms linear in u , one has

$$\frac{d^2u}{ds^2} + \frac{1}{\rho^2} \left\{ \left(1 - \frac{\Delta p}{p}\right) \left[\left(1 + \frac{X}{\rho}\right)^2 \rho k_{1M} g(X) + 2 \left(1 + \frac{X}{\rho}\right) b(X) \right] - 1 \right\} u = 0, \quad (11)$$

where k_1 has been replaced by k_{1M} to indicate that the measured gradient is to be used.

For comparison, when $\Delta p = 0$, Eq. (11) becomes

$$\frac{d^2u}{ds^2} + \frac{1}{\rho^2} (1 + \rho k_{1S}) u = 0, \quad (12)$$

where k_1 is now replaced by k_{1S} to indicate that the betatron frequencies in this case are obtained from the design parameters and were calculated using SYNCH.

Assuming that the motion described by Eq. (11) is not very different from that described by Eq. (12), one has for the change in the radial tune

$$\Delta\nu_x = \frac{1}{4\pi} \int_c (K_{xM}(s) - K_{xS}(s)) \cdot \beta_x(s) ds, \quad (13)$$

where K_{xM} and K_{xS} are the coefficients of u in Eqs. (11) and (12).

C. VERTICAL MOTION

For small betatron amplitudes and median plane symmetry, the vertical motion is described adequately by

$$\frac{d^2y}{ds^2} = - \frac{e}{p} \left(1 + \frac{x}{\rho}\right)^2 B_x. \quad (14)$$

But

$$B_x(x, y) = B_x(x, 0) + y \left(\frac{\partial B_x}{\partial y} \right)_{x, 0} + \dots \quad (15)$$

Using the ampere circuital law and median plane symmetry, one has

$$B_x(x, y) = y B_y'(x, 0). \quad (16)$$

Setting $x = X$ gives

$$\frac{d^2y}{ds^2} - \frac{1}{\rho} \left(1 - \frac{\Delta p}{p}\right) \left(1 + \frac{X}{\rho}\right)^2 k_{1M} g(X) y = 0. \quad (17)$$

For $\Delta p = 0$ and k_1 replaced by k_{1S} , Eq. (17) becomes

$$\frac{d^2y}{ds^2} - \frac{k_{1S}}{\rho} y = 0. \quad (18)$$

Again, assuming that the change from Eq. (18) to Eq. (17)

only causes a small tune shift

$$\Delta v_Y = \frac{1}{4\pi} \int_C (K_{YM} - K_{YS}) \beta_Y(s) ds, \quad (19)$$

where K_{YM} and K_{YS} are the coefficients of y in Eqs. (17) and (18).

D. HARD EDGE APPROXIMATION

Although Eqs. (13) and (19) are sufficient as expressed, one needs to know the focusing functions K_{xM} , K_{xS} , K_{yM} , K_{yS} as a function of position. This is most conveniently done by assuming them constant within each magnet and abruptly reduced to zero along some curve that represents the effective termination of the magnet. Justification for this procedure is obtained by appealing to the fact that the reduction in field from full value to zero occurs in a distance that is small compared with a betatron wavelength.

A further simplification is introduced. The curve representing the effective termination of the magnetic field at the entrance to the magnet is a mirror image of the termination curve at the exit end of the magnet. Analytically for one magnet, one has

$$B_Y(x, s) = B_Y(x) \cdot \left\{ S_1(s - s_1 + f(x)) - S_2(s - s_2 - f(x)) \right\}, \quad (20)$$

where S_1 and S_2 are step functions and

$$s = s_1 - f(x) \quad (21)$$

is the termination curve at the entrance end, and

$$s = s_2 + f(x) \quad (22)$$

is the termination curve at the exit end. For convenience

$$s_2 - s_1 = \text{physical magnet length}, \quad (23)$$

and also equals magnet length used in SYNCH. Equation (20) gives also

$$B_y'(x, s) = B_y'(x) \cdot \{s_1 - s_2\} + B_y(x) f'(x) \{\delta_1 + \delta_2\} \quad (24)$$

where δ_1 and δ_2 are delta functions corresponding to s_1 and s_2 .

E. EXPLICIT EXPRESSIONS

In this perturbation calculation the linear orbit functions $\beta_x(s)$, $\beta_y(s)$, and $x_p(s)$ are obtained from the SYNCH program. The periodic solution for the off momentum closed orbit is given then by

$$x(s) = x_p(s) \cdot \frac{\Delta p}{p} \quad (25)$$

For convenience, let¹

$$K_{xM} = \frac{1}{\rho^2} \left\{ \left(1 - \frac{\Delta p}{p}\right) \left[\left(1 + \frac{x}{\rho}\right)^2 \rho k_{1M} g(x) + 2 \left(1 + \frac{x}{\rho}\right) b(x) \right] - 1 \right\} \quad (26)$$

$$K_{xS} = \frac{1}{\rho^2} (1 + \rho k_{1S}) \quad (27)$$

$$K_{yM} = -\frac{1}{\rho} \left(1 - \frac{\Delta p}{p}\right) \left(1 + \frac{x}{\rho}\right)^2 k_{1M} g(x) \quad (28)$$

$$K_{yS} = -\frac{1}{\rho} k_{1S} \quad (29)$$

$$L_{xM} = \frac{1}{\rho} \left(1 - \frac{\Delta p}{p}\right) \left(1 + \frac{x}{\rho}\right)^2 b(x) \quad (30)$$

$$L_{xS} = \frac{1}{\rho} \quad (31)$$

$$L_{YM} = -\frac{1}{\rho} \left(1 - \frac{\Delta p}{p}\right) \left(1 + \frac{X}{\rho}\right)^2 b(X) \quad (32)$$

$$L_{YS} = -\frac{1}{\rho} \quad (33)$$

$$f_{MF} = \Delta S_F + A_F X + B_F X^2 + C_F X^3 + \dots \quad (34)$$

$$f_{MD} = \Delta S_D + A_D X + B_D X^2 + C_D X^3 + \dots \quad (35)$$

$$f_{SF} = A_{SF} X \quad (36)$$

$$f_{SD} = A_{SD} X. \quad (37)$$

The coefficients A_{SF} and A_{SD} are determined such that the effective magnet end shape for the SYNCH run is identical with the physical magnet end. The remaining coefficients in Eqs. (34) and (35) are to be chosen subsequently.

In terms of these symbols, the tune shifts for the booster lattice whose period is N becomes

$$\begin{aligned} \Delta v_x = \frac{2N}{4\pi} & \left\{ \int_{s_{1F}}^{s_{2F}} (K_{xM} - K_{xS}) \beta_x ds + \int_{s_{1D}}^{s_{2D}} (K_{xM} - K_{xS}) \beta_x ds \right. \\ & + \left[(K_{xM} \beta_x)_{\text{entr.}(F)} + (K_{xM} \beta_x)_{\text{exit}(F)} \right] \Delta S_F \\ & + \left[(K_{xM} \beta_x)_{\text{entr.}(D)} + (K_{xM} \beta_x)_{\text{exit}(D)} \right] \Delta S_D \\ & + (L_{xM} \beta_x^{f'M})_{\text{entr.}(F)} + (L_{xM} \beta_x^{f'M})_{\text{exit}(F)} \\ & + (L_{xM} \beta_x^{f'M})_{\text{entr.}(D)} + (L_{xM} \beta_x^{f'M})_{\text{exit}(D)} \\ & - (L_{xS} \beta_x^{f'S})_{\text{entr.}(F)} - (L_{xS} \beta_x^{f'S})_{\text{exit}(F)} \\ & \left. - (L_{xS} \beta_x^{f'S})_{\text{entr.}(D)} - (L_{xS} \beta_x^{f'S})_{\text{exit}(D)} \right\} \quad (38) \end{aligned}$$

and

$$\begin{aligned}
\Delta v_Y = \frac{2N}{4\pi} & \left\{ \int_{s_{1F}}^{s_{2F}} (K_{YM} - K_{YS}) \beta_Y ds + \int_{s_{1D}}^{s_{2D}} (K_{YM} - K_{YS}) \beta_Y ds \right. \\
& + \left[(K_{YM} \beta_Y)_{\text{entr.}(F)} + (K_{YM} \beta_Y)_{\text{exit}(F)} \right] \Delta S_F \\
& + \left[(K_{YM} \beta_Y)_{\text{entr.}(D)} + (K_{YM} \beta_Y)_{\text{exit}(D)} \right] \Delta S_D \\
& + (L_{YM} \beta_Y^{f'M})_{\text{entr.}(F)} + (L_{YM} \beta_Y^{f'M})_{\text{exit}(F)} \\
& + (L_{YM} \beta_Y^{f'M})_{\text{entr.}(D)} + (L_{YM} \beta_Y^{f'M})_{\text{exit}(D)} \\
& - (L_{YS} \beta_Y^{f'S})_{\text{entr.}(F)} - (L_{YS} \beta_Y^{f'S})_{\text{exit}(F)} \\
& \left. - (L_{YS} \beta_Y^{f'S})_{\text{entr.}(D)} - (L_{YS} \beta_Y^{f'S})_{\text{exit}(D)} \right\} \quad (39)
\end{aligned}$$

Note that s_{1F} , s_{2F} , s_{1D} , s_{2D} are the effective magnet ends on the central orbit as used in SYNCH. Thus, positive ΔS_F and ΔS_D indicate that the effective magnet ends at the central orbit increase the magnet length in the perturbed case.

F. OPTIMUM END SHAPES

Equations (38) and (39) show that the tune shifts Δv_x and Δv_y away from the corresponding SYNCH tunes are linearly related to the coefficients in the power series expansion of the effective end shapes as given in Eqs. (34) and (35). One might consider, therefore, that an optimum end shape could be obtained by adjusting ΔS_F , A_F , B_F , C_F , etc., and ΔS_D , A_D , B_D , C_D , etc., such that the quantity

$$\int (w_x \left(\frac{\Delta p}{p}\right) \cdot (\Delta v_x)^2 + w_y \left(\frac{\Delta p}{p}\right) \cdot (\Delta v_y)^2) d\left(\frac{\Delta p}{p}\right) = \text{minimum}. \quad (40)$$

In this way any design or fabrication difficulties in the body of the magnet could be rectified by finding suitable end shaping that yields the desired effective end shape. Notice, however, that, although this procedure will work, one should be careful about interpreting the ΔS_F , ΔS_D , A_F , A_D so obtained. The difficulty stems from the fact that, in the linear theory, additional focusing may be obtained either by increasing the magnet length or by changing the edge angle. The functions of momentum that multiply ΔS_F or ΔS_D are only negligibly different from those that multiply A_F and A_D . If they had been identical, the least squares procedure would have failed. To obtain realistic results, it is preferable to remove this difficulty by choosing fixed values for ΔS_F and ΔS_D and minimize Eq. (40) with respect to the remaining coefficients.

G. LEAST SQUARES ANALYSIS

In Eq. (38) let the quantities not subject to adjustment be designated by $DNUX(J)$ where uniformly incremented values of $\Delta p/p$ are represented by the index J . Thus

$$\begin{aligned}
 \text{DNUX}(J) = \frac{2N}{4\pi} & \left\{ \int_{s_{1F}}^{s_{2F}} (K_{xM} - K_{xS}) \beta_x ds + \int_{s_{1D}}^{s_{2D}} (K_{xM} - K_{xS}) \beta_x ds \right. \\
 & + \left[(K_{xM} \beta_x)_{\text{entr.}(F)} + (K_{xM} \beta_x)_{\text{exit}(F)} \right] \Delta S_F \\
 & + \left[(K_{xM} \beta_x)_{\text{entr.}(D)} + (K_{xM} \beta_x)_{\text{exit}(D)} \right] \Delta S_D \\
 & - (L_{xS} \beta_x^{f'S})_{\text{entr.}(F)} - (L_{xS} \beta_x^{f'S})_{\text{exit}(F)} \\
 & \left. - (L_{xS} \beta_x^{f'S})_{\text{entr.}(D)} - (L_{xS} \beta_x^{f'S})_{\text{exit}(D)} \right\} \quad (41)
 \end{aligned}$$

By utilizing Eqs. (34) and (35) and defining the array $D(K)$ to be

$$\{D(K)\} = \{A_F, A_D, B_F, B_D, C_F, C_D, \dots\} \quad (42)$$

and the array $T(J,K)$ to be

$$\begin{aligned}
 T(J,1) &= (L_{xM} \beta_x)_{\text{entr.}(F)} + (L_{xM} \beta_x)_{\text{exit}(F)} \\
 T(J,2) &= (L_{xM} \beta_x)_{\text{entr.}(D)} + (L_{xM} \beta_x)_{\text{exit}(D)} \\
 T(J,3) &= 2(L_{xM} \beta_x^X)_{\text{entr.}(F)} + 2(L_{xM} \beta_x^X)_{\text{exit}(F)} \\
 T(J,4) &= 2(L_{xM} \beta_x^X)_{\text{entr.}(D)} + 2(L_{xM} \beta_x^X)_{\text{exit}(D)} \\
 T(J,5) &= 3(L_{xM} \beta_x^{X^2})_{\text{entr.}(F)} + 3(L_{xM} \beta_x^{X^2})_{\text{exit}(F)} \\
 T(J,6) &= 3(L_{xM} \beta_x^{X^2})_{\text{entr.}(D)} + 3(L_{xM} \beta_x^{X^2})_{\text{exit}(D)} \\
 T(J,7) &= \text{etc.,} \quad (43)
 \end{aligned}$$

Equation (38) becomes

$$\Delta v_x(J) = DNUX(J) + \sum_K T(J,K)D(K). \quad (44)$$

In an analagous manner let the fixed quantities in Eq. (39) be designated by DNUY(J). Then

$$\begin{aligned} DNUY(J) = \frac{2N}{4\pi} & \left\{ \int_{s_{1F}}^{s_{2F}} (K_{YM} - K_{YS}) \beta_Y ds + \int_{s_{1D}}^{s_{2D}} (K_{YM} - K_{YS}) \beta_Y ds \right. \\ & + \left[(K_{YM} \beta_Y)_{entr.(F)} + (K_{YM} \beta_Y)_{exit(F)} \right] \Delta S_F \\ & + \left[(K_{YM} \beta_Y)_{entr.(D)} + (K_{YM} \beta_Y)_{exit(D)} \right] \Delta S_D \\ & - (L_{YS} \beta_Y^{f's})_{entr(F)} - (L_{YS} \beta_Y^{f's})_{exit(F)} \\ & \left. - (L_{YS} \beta_Y^{f's})_{entr.(D)} - (L_{YS} \beta_Y^{f's})_{exit(D)} \right\}. \quad (45) \end{aligned}$$

Further, let the array S(J,K) be

$$\begin{aligned} S(J,1) &= (L_{YM} \beta_Y)_{entr.(F)} + (L_{YM} \beta_Y)_{exit(F)} \\ S(J,2) &= (L_{YM} \beta_Y)_{entr.(D)} + (L_{YM} \beta_Y)_{exit(D)} \\ S(J,3) &= 2(L_{YM} \beta_Y^X)_{entr.(F)} + 2(L_{YM} \beta_Y^X)_{exit(F)} \\ S(J,4) &= 2(L_{YM} \beta_Y^X)_{entr.(D)} + 2(L_{YM} \beta_Y^X)_{exit(D)} \\ S(J,5) &= 3(L_{YM} \beta_Y^{X^2})_{entr.(F)} + 3(L_{YM} \beta_Y^{X^2})_{exit(F)} \\ S(J,6) &= 3(L_{YM} \beta_Y^{X^2})_{entr.(D)} + 3(L_{YM} \beta_Y^{X^2})_{exit(D)} \\ S(J,7) &= \text{etc.} \end{aligned} \quad (47)$$

Equation (39) then becomes

$$\Delta v_y(J) = DNUY(J) + \sum_K S(J,K)D(K) \quad (48)$$

If Eqs. (44) and (48) are substituted into Eq. (40) and the minimization carried out one finds for D(K)

$$D(K) = - \sum_L C^{-1}(K,L)A(L) \quad (49)$$

where

$$A(L) = \sum_J (W_x(J)DNUX(J)T(J,L) + W_y(J)DNUY(J)S(J,L)), \quad (50)$$

and

$$C(K,L) = \sum_J (W_x(J)T(J,K)T(J,L) + W_y(J)S(J,K)S(J,L)). \quad (51)$$

Equation (40) at the minimum becomes

$$SUM = \sum_J (W_x(J)DNUX^2(J) + W_y(J)DNUY^2(J)) + \sum_K A(K)D(K). \quad (52)$$

The operations indicated in Eqs. (40) to (52) have been coded in the program TUNA. In order to obtain the inverse matrix, MATINV by Garbow² has been included as a subroutine.

H. NUMERICAL RESULTS FOR BOOSTER

All numerical results are expressed in the coordinate system (x,y,s) where s is distance measured along the equilibrium orbit for $p = p_0$, x is measured in the direction radially normal to the equilibrium orbit, and y is the vertical direction. The fractional momentum change $\Delta p/p$ is converted to equilibrium orbit position at the entrance to the

F-magnet.

Ideal design gradients as a function of x were chosen previously³ and are characterized by a selection of sextupole moments, $k_2(F) = 0.6079\text{m}^{-2}$, $k_2(D) = -1.256\text{m}^{-2}$. Figure 1 indicates the variation of the idealized gradients with x . Figure 2 shows that both the radial and vertical tune variation with momentum has indeed been reduced to zero. In addition, the increment in the gradient length at each end of the F and the D magnets is shown. This was obtained by fixing $\Delta S_F = \Delta S_D = 0$ and using the least squares adjustment to find the coefficients A_F , A_D , B_F , B_D , etc. The incremental gradient lengths so obtained correspond to an effective termination of the magnetic fields characterized principally by $A_F = -0.0354$, $A_D = -0.0301$, the conditions that make the end faces parallel.

The normalized gradients at 8 GeV excitation measured by R. E. Peters⁴ are shown in Figure 3. These gradients together with the effective termination used in the magnet design, namely, that the effective entrance and exit planes of the magnet are parallel and coincide with the end laminations, yield tune variations as shown in Figure 4. Clearly the effects of the finite pole width cause fluctuations in the gradient that are reflected in the tune variations.

In order to realize the design effective endings for the magnets, end packs were machined by numerically controlled contour milling. The surfaces chosen were derived basically

from two-dimensional reasoning,⁵ the variation with the radial dimension being introduced in such a manner as to permit the surface to match the design body contours smoothly. The effective termination of the magnetic fields after installation of these end packs was measured by Peters.⁴ Figure 5 shows the variation of the tunes with momentum for this case in which measured gradients and measured field terminations are employed. It is clear that the end packs have over compensated for the difficulty shown in Figure 4.

Figure 6 shows the result of asking the question, "What is the best shape for the effective field termination?" The least squares minimization mode of TUNA was activated using the measured values $\Delta S_F = 0.007689$ m and $\Delta S_D = 0.01162$ m for each of several polynomial degrees from 4 through 9. Only the results for an eighth degree fit are shown since all lower degrees gave tune variations outside of the band ± 0.1 . Also shown are the incremental gradient lengths that are derived from the eighth order effective termination shapes.

Table 1 presents the power series coefficients that express the shape of the effective magnetic field terminations according to Eqs. (34) and (35). Three cases are shown for each magnet; (1) measured gradients-design terminations, (2) measured gradients-measured terminations, (3) measured gradients-adjusted terminations. Table 2 presents the numerical calculation of the radial tune variation with momentum for each of the cases just mentioned and in addition the test case

in which the idealized gradient was used together with the design termination. Table 3 gives the same information as Table 2 except that it relates to the vertical tune.

In summary, then, the measurements of curves along which the interior fields of the magnets effectively terminate show that the simplified method of deriving an end pack shape needs modification. To date, a method of using the difference between the measured terminating curve and the desired terminating curve to generate a new iron shape has been devised. Its basic limitation stems from the fact that the pole width is larger than the aperture width and, hence, it is impossible to determine completely the pole shape. This problem is being considered further.

Subject

IDEAL NORMALIZED GRADIENTS

$$k_1(F) = 2.2147 \text{ m}^{-1}$$

$$k_1(D) = -2.7719 \text{ m}^{-1}$$

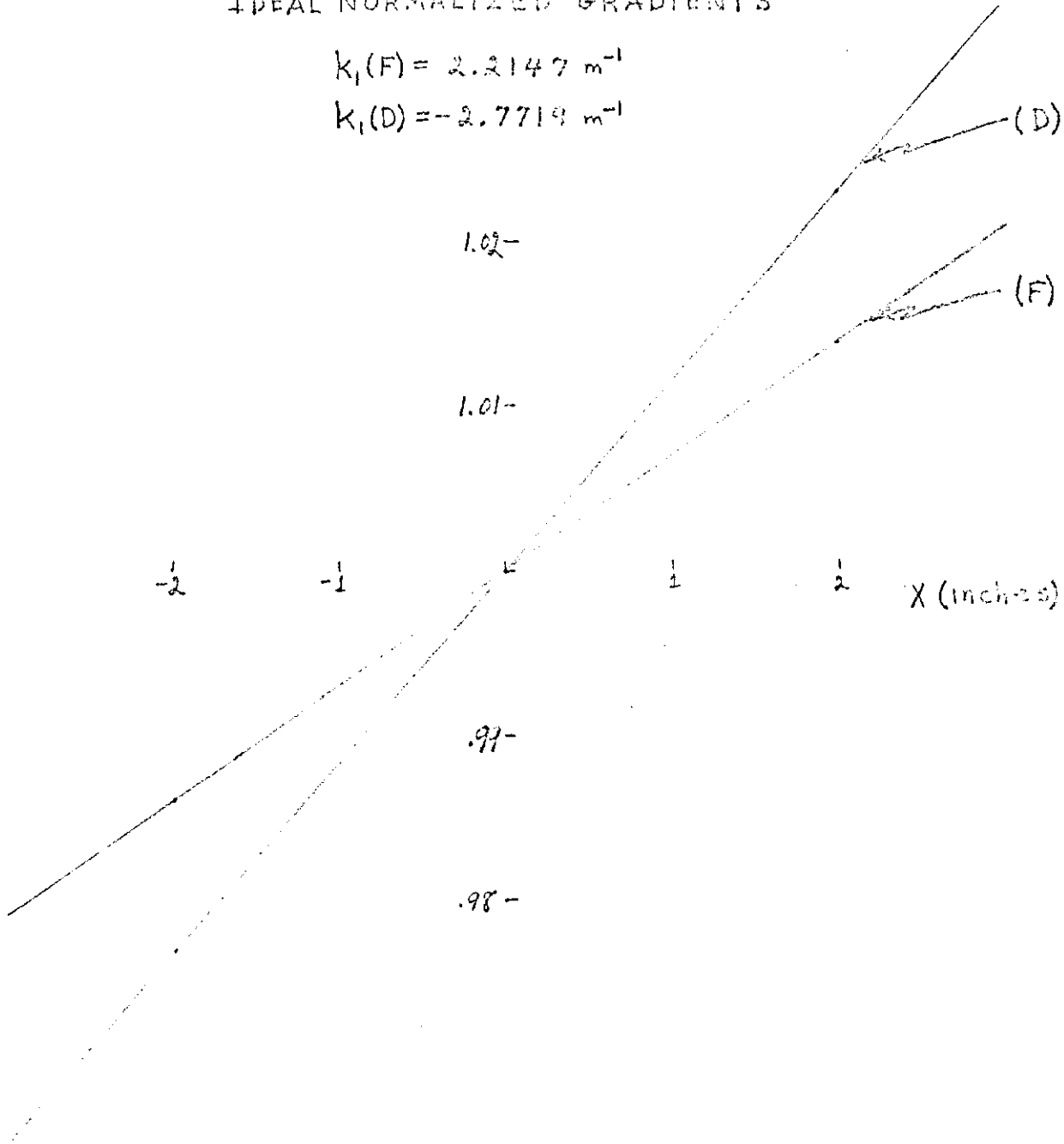


FIG. 1

 national accelerator laboratory	Author	Section	Page 16 of 24
	Date	Category TUNA	Serial FN-192 0300

Subject

BETATRON FREQUENCY SHIFT VS. MOMENTUM SHIFT
IDEAL GRADIENTS
DESIGN ENDS

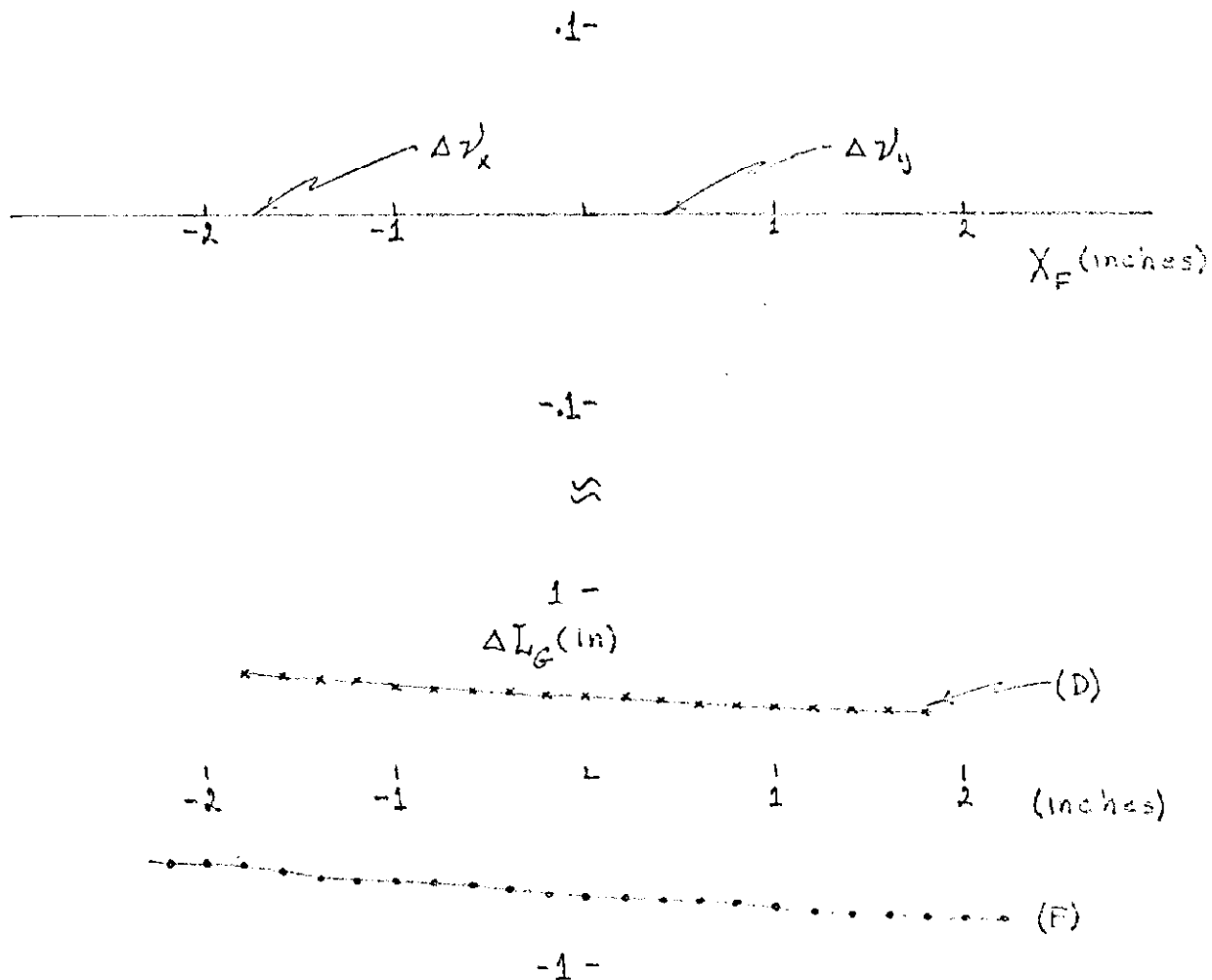


FIG. 2

Subject

MEASURED NORMALIZED GRADIENTS (PETERS)

$$k_1(F) = 2.2006 \text{ m}^{-1}$$

$$k_1(D) = -2.7627 \text{ m}^{-1}$$

$$B_0(F) = 7259 \text{ G}$$

$$B_0(D) = 6152 \text{ G}$$

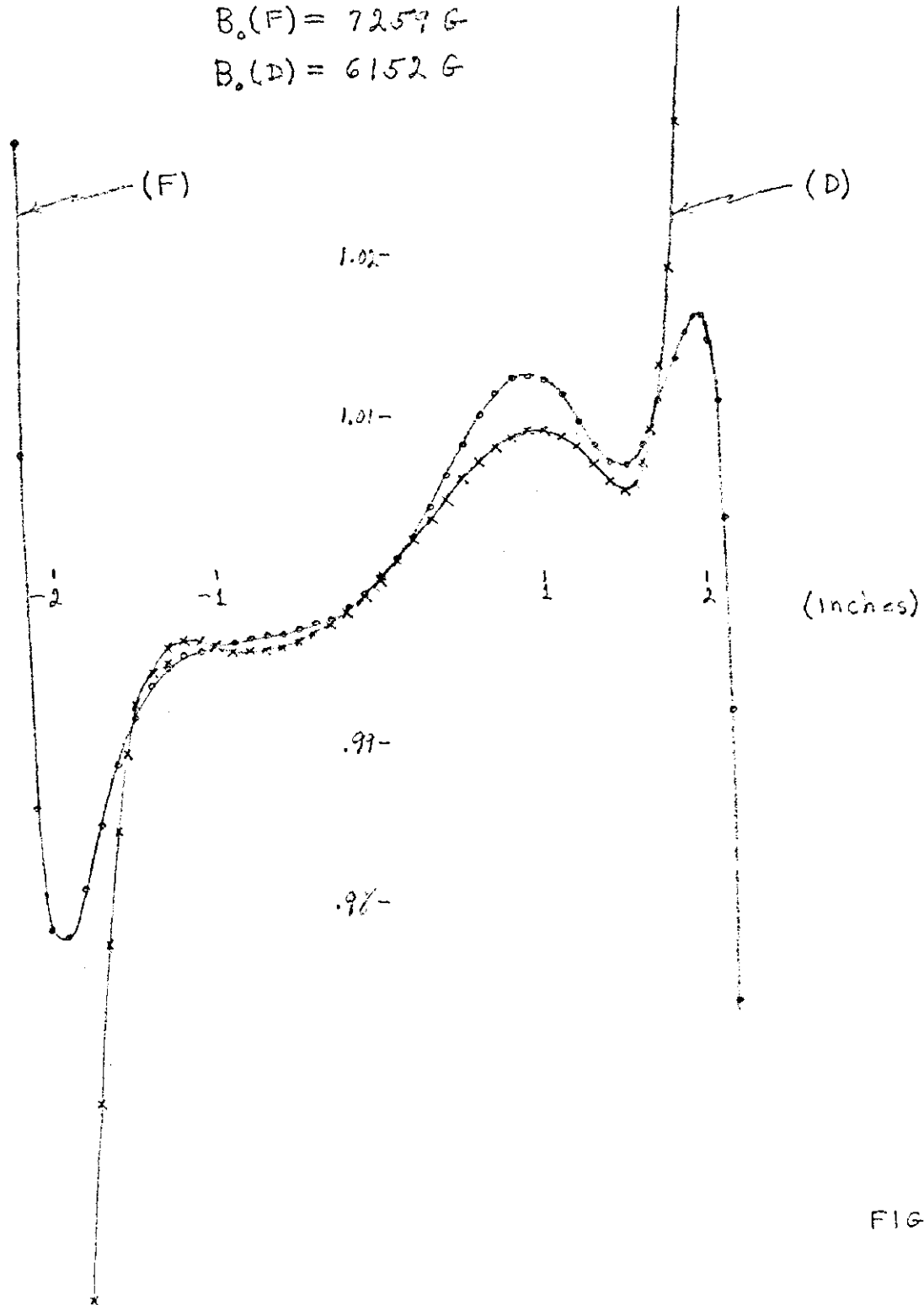


FIG. 3

 national accelerator laboratory	Author	Section	Page 18 of 24
	Date 11/12/67	Category TUNA	Serial FN-192 0300

Subject

BETATRON FREQUENCY SHIFT VS. MOMENTUM SHIFT
 MEASURED GRADIENTS (PETERS)
 DESIGN ENDS

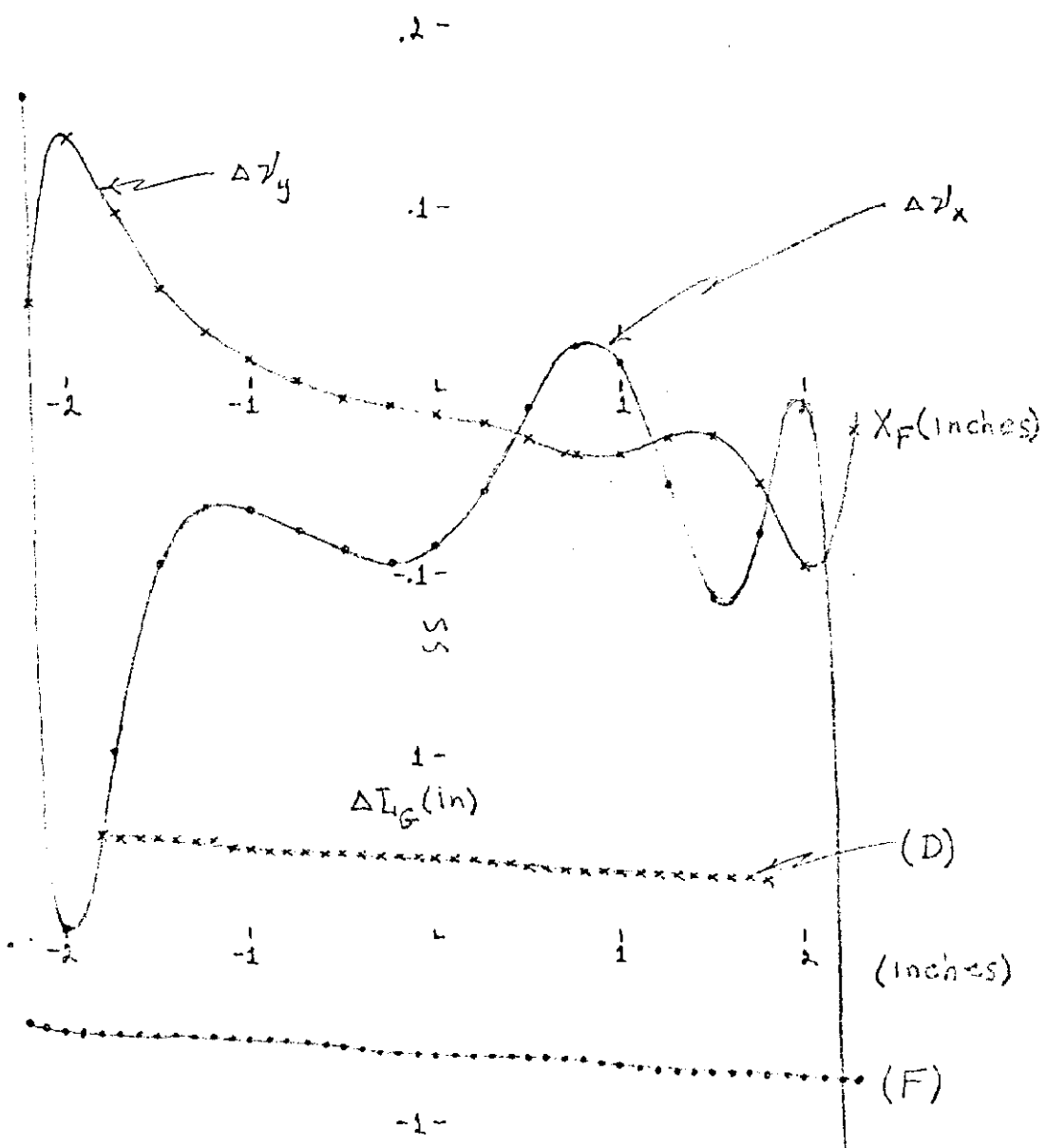


FIG. 4

 national accelerator laboratory	Author	Section	Page 19 of 24
	Date 11/12/68	Category TUNA	Serial FN-192 0300

Subject

BETATRON FREQUENCY SHIFT VS. MOMENTUM SHIFT

MEASURED GRADIENTS (PETERS)
MEASURED ENDS (PETERS)

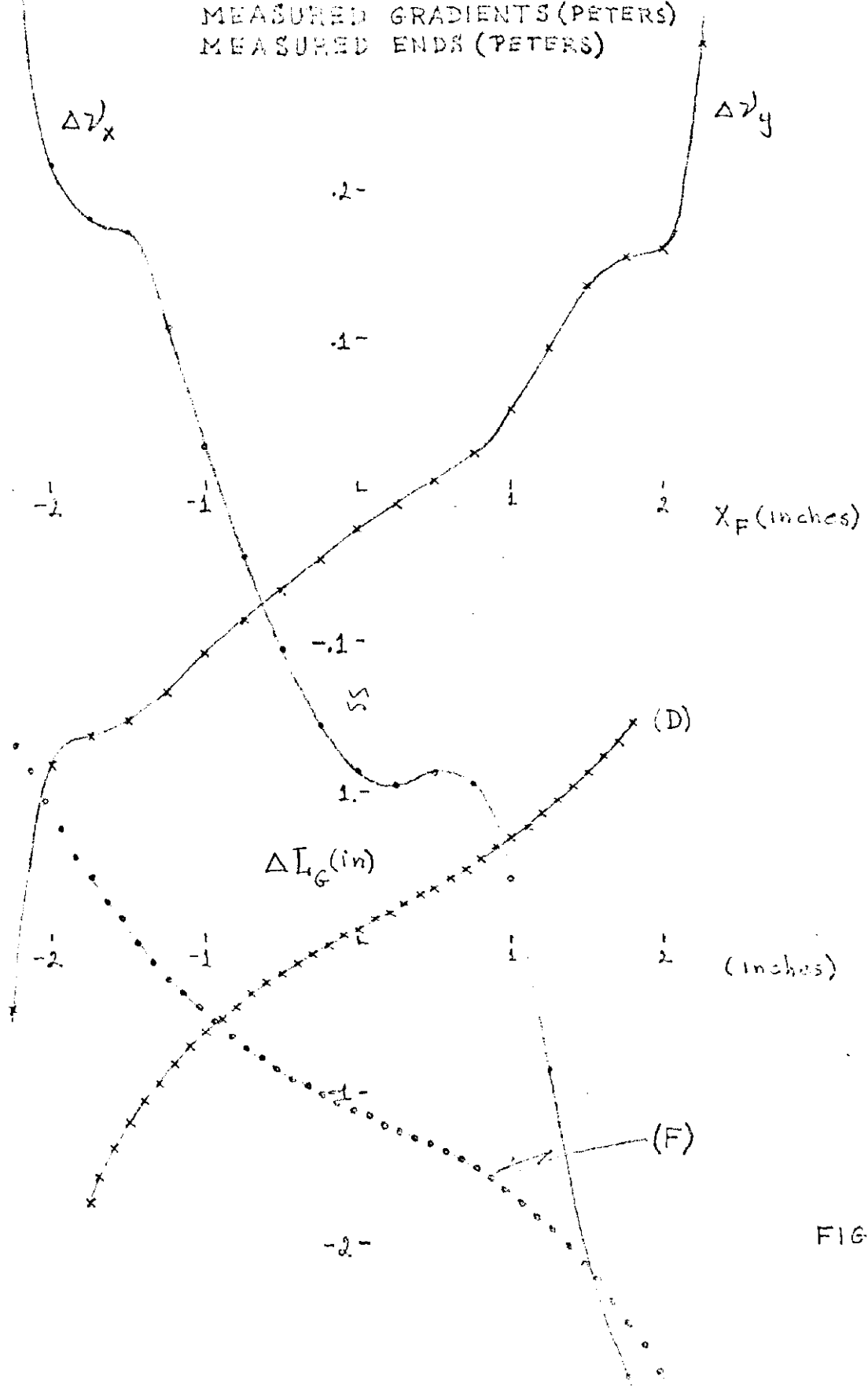


FIG. 5

 national accelerator laboratory	Author	Section	Page 20 of 24
	Date 11/12/64	Category TUNA	Serial FN-192 0300

Subject

BETATRON FREQUENCY SHIFT VS. MOMENTUM SHIFT
MEASURED GRADIENTS (PETERS)
ADJUSTED ENDS

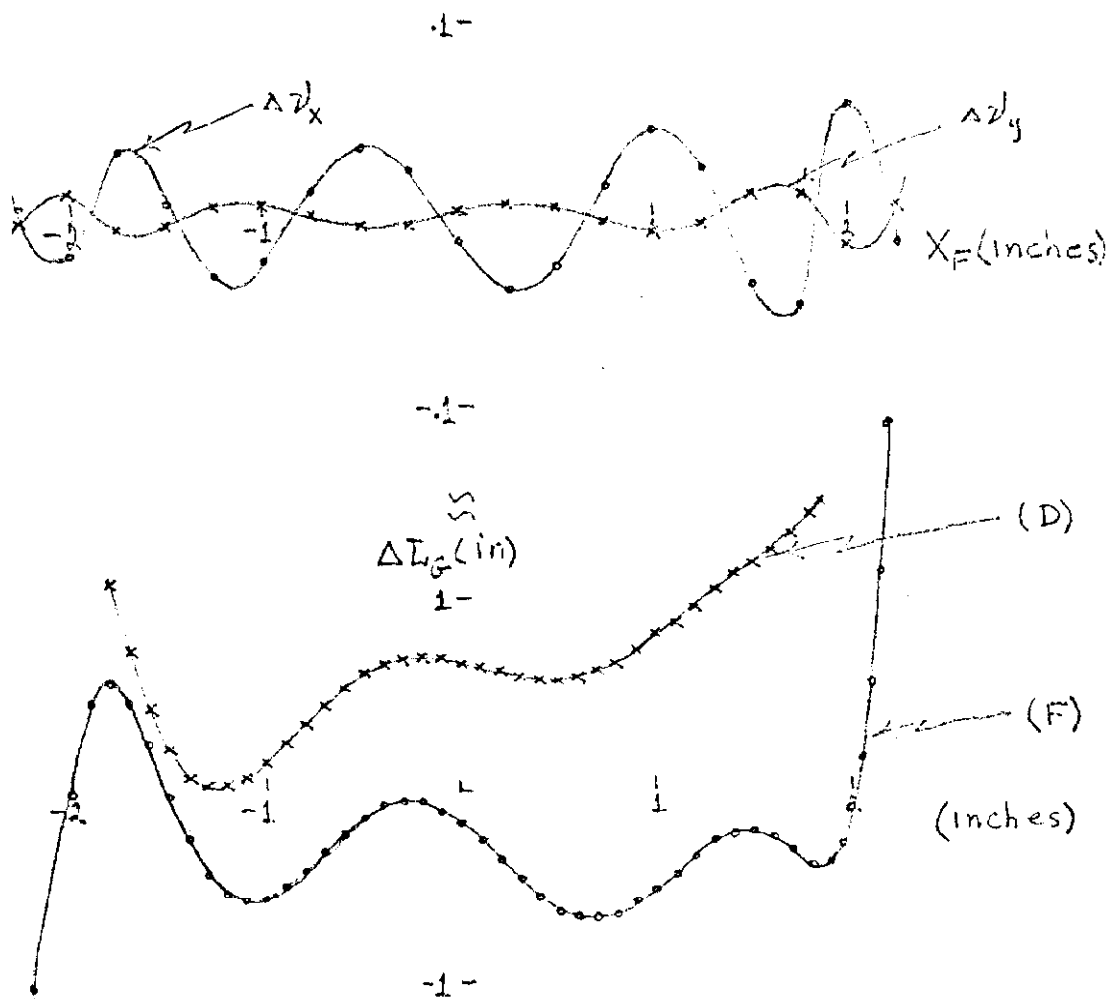


FIG. 6

Table 1. Coefficients for Effective Field Termination

$$s_2 - s_1 = 2.8896m$$

	<u>F-Magnet</u>			<u>D-Magnet</u>		
	Design	Meas.*	Adjusted	Design	Meas.*	Adjusted
$\Delta S(m)$	0.0000	0.007689	0.007689	0.0000	0.01162	0.01162
A	-0.0354	-0.08110	-0.03189	-0.0301	0.02378	-0.01501
$B(m^{-1})$		-0.3560	-0.9852		-0.6844	0.2758
$C(m^{-2})$		2.300	-0.1230E+2		-1.313	0.1265E+2
$D(m^{-3})$		-0.1065E+3	0.1464E+4		-110.8	-0.9467E+3
$E(m^{-4})$			0.7149E+4			-0.6376E+4
$F(m^{-5})$			-0.7240E+6			0.4329E+6
$G(m^{-6})$			-0.9612E+6			0.2041E+6
$H(m^{-7})$			0.1132E+9			-0.6190E+8

*R. E. Peters

Table 2. Radial Betatron Frequency Variation with Momentum

SYNCH tune = 6.700

$\frac{\Delta p}{p}$	Design Grad. Design Ends.	Meas. Grad.* Design Ends.	Meas. Grad.* Meas. Ends.*	Meas. Grad.* Adjusted Ends
-0.018	0.000	0.160	0.836	0.003
-0.016	0.000	-0.297	0.217	-0.020
-0.014	0.000	-0.199	0.181	0.033
-0.012	0.000	-0.096	0.172	0.006
-0.010	0.000	-0.065	0.109	-0.031
-0.008	0.000	-0.068	0.029	-0.023
-0.006	0.000	-0.078	-0.045	0.012
-0.004	0.000	-0.088	-0.106	0.035
-0.002	0.000	-0.093	-0.156	0.022
0.00	0.000	-0.085	-0.187	-0.013
0.002	0.000	-0.056	-0.195	-0.039
0.004	0.000	-0.010	-0.188	-0.027
0.006	0.000	0.025	-0.196	0.015
0.008	0.000	0.013	-0.259	0.045
0.010	0.000	-0.051	-0.386	0.024
0.012	0.000	-0.113	-0.525	-0.037
0.014	0.000	-0.080	-0.589	-0.048
0.016	0.000	-0.009	-0.638	0.059
0.018	0.000	-0.589	-1.367	-0.016

*R. E. Peters

Table 3. Vertical Betatron Frequency Variation with Momentum

SYNCH tune = 6.800

$\frac{\Delta p}{p}$	Design Grad. Design Ends.	Meas. Grad.* Design Ends.	Meas. Grad.* Meas. Ends.*	Meas. Grad.* Adjusted Ends
-0.018	0.000	0.048	-0.343	-0.003
-0.016	0.000	0.138	-0.182	0.011
-0.014	0.000	0.096	-0.163	-0.008
-0.012	0.000	0.054	-0.153	-0.005
-0.010	0.000	0.031	-0.133	0.004
-0.008	0.000	0.016	-0.110	0.006
-0.006	0.000	0.005	-0.088	0.000
-0.004	0.000	-0.003	-0.068	-0.005
-0.002	0.000	-0.009	-0.047	-0.004
0.000	0.000	-0.012	-0.027	0.002
0.002	0.000	-0.019	-0.009	0.006
0.004	0.000	-0.027	0.006	0.004
0.006	0.000	-0.035	0.024	-0.004
0.008	0.000	-0.035	0.053	-0.009
0.010	0.000	-0.027	0.094	-0.003
0.012	0.000	-0.025	0.135	0.010
0.014	0.000	-0.051	0.154	0.010
0.016	0.000	-0.097	0.160	-0.016
0.018	0.000	-0.021	0.297	0.005

*R. E. Peters

REFERENCES

1. Note that near the magnet ends one does not know a priori whether to use the curvilinear coordinate system or a rectangular coordinate system until the actual location of the effective termination of the magnetic field has been found. Assuming that the terminating surface is about 1 centimeter from the last lamination, an estimate of the uncertainty introduced into the tune calculations in using Eqs. (26) and (28) instead of their cartesian equivalents is approximately 0.001. This effect is therefore neglected.
2. Matrix Inversion with Accompanying Solution of Linear Equations, Burton S. Garbow, Argonne National Laboratory Report AN-F402, February 23, 1959.
3. Determination of Booster Magnet Sextupole Strength, S. C. Snowdon, TM-156, March 4, 1969.
4. R. E. Peters, private communication.
5. Magnet End Termination, S. C. Snowdon, FN-184, April 29, 1969.